Tempo and Mode of Evolutionary Radiation in Iguanian Lizards

Luke J. Harmon,* James A. Schulte II,† Allan Larson, Jonathan B. Losos

Identification of general properties of evolutionary radiations has been hindered by the lack of a general statistical and phylogenetic approach applicable across diverse taxa. We present a comparative analytical framework for examining phylogenetic patterns of diversification and morphological disparity with data from four iguanian-lizard taxa that exhibit substantially different patterns of evolution. Taxa whose diversification occurred disproportionately early in their evolutionary history partition more of their morphological disparity among, rather than within, subclades. This inverse relationship between timing of diversification and morphological disparity within subclades may be a general feature that transcends the historically contingent properties of different evolutionary radiations.

Evolutionary radiation—cladogenesis accompanied by ecological and morphological disparity among lineages—has been studied for more than a century (*1*–*3*). Recent debate has centered on whether general rules characterize patterns of radiation or whether evolutionary divergence is largely idiosyncratic and group-specific (*4*, *5*). A comparative approach capable of revealing generalities that transcend individual radiations has been difficult to find, particularly for radiations lacking extensive paleontological documentation. However, new methods allow patterns of cladogenesis to be examined using phylogenetic hypotheses of extant species (*6*), and methods developed by paleontologists for quantifying ecomorphological disparity may be extended to neontological studies (*7*–*10*). Integrating and extending these methods, we present a comparative phylogenetic approach to identify general patterns in the relationship between cladogenesis and the evolution of morphological disparity among evolutionary radiations.

Paleontological and molecular-systematic analyses suggest that the initial stages of evolutionary radiation often show extensive cladogenesis and rapid ecological and morphological divergence among lineages, often leading to long-term persistence of among-lineage ecomorphological differences (*2*, *7*). Nonetheless, increases in species richness and ecomorphological disparity are not always restricted to an early phase of radiation (*7*–*10*), and extensive ecomorphological convergence may occur among lineages (*11*, *12*). Consequently, three questions deserve further attention: (i) Is the origin of extant lineages concentrated disproportionately early in the history of an evolutionary radiation? (ii) How is morphological disparity partitioned within versus among subclades throughout the phylogenetic history of a radiation? (iii) Is morphological diversification within a radiating clade related to the temporal pattern of cladogenesis?

We examined four clades of iguanian lizards that are species-rich, ecologically and morphologically diverse, and similar in time of origin and many aspects of natural history, morphology, and ecology: Caribbean *Anolis* (*13*), *Liolaemus* (*14*, *15*), Australian agamids (*16*, *17*), and phrynosomatines (*18*). For each taxon, we used a phylogeny based on molecular data (*19*) to examine historical patterns of extant subclades. The tempo of increase in species richness, a function of both speciation and extinction, was examined with lineage-through-time plots (*6*). The lineage diversity index (LDI) estimates the extent to which the rate of lineage accumulation departs from a stochastic model of constant rates of diversification per lineage; a positive value indicates that a taxon experienced greater than expected rates of increase in lineage number early in its history. To calculate the LDI for each clade, we quantified the overall departure of diversification rate from that expected under a simple pure-birth model. We first constructed the null expectation under such a model by connecting with a straight line the point representing the first node in the phylogeny with the point representing the present number of lineages on the log-linear lineage accumulation curve. This result represents the null hypothesis of exponential growth of lineages under a pure-birth model. We then found the area between this null model and the actual accumulation plot for the clade, with positive values for the area when the accumulation plot was above that of the null model and negative when it was below. We used this area as a measure of departure from the null model. Because recent nodes from the phylogeny may be missing, we calculated the area underlying only the first two-thirds of each phylogeny in this and subsequent analyses. These LDI values were corroborated with the γ statistic, which tests for homogeneity of the diversification rate through time (*20*, *21*).

To examine the history of morphological variation, we took measurements for as many of the species included in the phylogenies as possible (*19*). Characters examined were ones for which variation among species is likely to represent adaptation to differences in habitat use, on the basis of previous field and laboratory studies (*22*). To examine the time course of morphological diversification, we calculated disparity-through-time plots. Disparity was calculated from average pairwise Euclidean distances between species, a variance-related method of estimating the dispersion of points in multivariate space that is insensitive to sample size (*10*). For each phylogeny, we first calculated disparity for the entire clade and then for each subclade defined by a node in that phylogeny. Relative disparities for each subclade were standardized by dividing a subclade's disparity by the disparity of the entire clade. To investigate patterns of disparity through time, we moved up the phylogeny from the root. At each divergence event (i.e., each node), we calculated the mean relative disparity for that point in time as the average of the relative disparities of all subclades whose ancestral lineages were present at that time. Values near 0 imply that subclades contain relatively little of the variation present within the taxon as a whole and that, consequently, most variation is partitioned as among-subclade differences; conversely, values near 1 imply that subclades contain a substantial proportion of the total variation and thus are likely to overlap extensively, indicating that subclades have independently evolved to occupy similar regions of morphological space. In this way, we plotted an average disparity through time analogous to the plots of lineage accumulation through time (see figs. S1 to S4 for a worked example), while avoiding the difficulties of inferring ancestral character states (*23*, *24*).

To calculate how much mean disparity differed from that expected under a null hypothesis of character evolution by unconstrained Brownian motion, we conducted 1000 simulations of morphological diversification on each taxon's phylogeny (*25*). [(We

Department of Biology, Campus Box 1137, Washington University, St. Louis, MO 63130–4899, USA.

*To whom correspondence should be addressed. E-mail: harmon@biology.wustl.edu

†Present address: Division of Amphibians and Reptiles, Post Office Box 37012, MRC 162, National Museum of Natural History, Smithsonian Institution, Washington, DC 20013–7012, USA.

also conducted simulations with a speciational model of character evolution; results were qualitatively unchanged (fig. S5).] Variances of each morphological axis among species in simulations were set equal to the actual variances of the principal components for each taxon. The morphological disparity index (MDI), the overall difference in relative disparity of a clade compared with that expected under the null hypothesis, was calculated as the area contained between the line connecting observed relative disparity points versus the line connecting median relative disparity points of the simulations; areas in which observed values were above expected were given positive values, whereas those below expected were given negative values. Results from this analysis were corroborated with the δ statistic, which tests for acceleration or deceleration of morphological change through time against a null model of constant rates of character evolution (*26*).

An early origin of many lineages occurs for three of the four lizard taxa. The lineage-accumulation curve for *Liolaemus* is fairly straight, indicating a steady increase in lineage accumulation through time, whereas Australian agamids show two bursts of diversification, one very early in the taxon's history and another more recently (Fig. 1). *Anolis* and phrynosomatines also exhibit elevated levels of early diversification, although less so than agamids. These results are supported by the γ statistic, which indicates a significant slowing through time in the rate of lineage accumulations in all clades except *Liolaemus* (Table 1). These results are robust to relaxation of the assumptions of the pure-birth model and are not affected by differences in species sampling among clades (figs. S6 and S7).

Disparity-through-time plots (Fig. 2) show that *Liolaemus* has high levels of average subclade disparity, whereas agamids have low average subclade disparity. These results indicate that subclades of *Liolaemus* have diversified greatly and substantially overlap each other in morphospace occupation. By contrast, most variation in agamids occurs among subclades, which occupy small and more isolated regions of morphological space. Anoles are again intermediate, as are phrynosomatines. These results are concordant with results from the δ statistic (*26*), for which Australian agamids and *Liolaemus* show extreme values and anoles and phrynosomatines are intermediate (Table 1).

A strong negative relationship exists between tempo of lineage diversification (LDI) and pattern of morphological radiation (MDI) (Fig. 3), a result strongly supported by a variety of null models (*19*) (figs. S6 and S7) and not affected by relaxation of the assumptions of a gradual mode of character evolution (fig. S5) or of a pure-birth model of species diversification (fig. S6), nor by the sampling of species in the analysis (*19*) (fig. S7). This result indicates that taxa with steady rates of increase in species richness tend to exhibit extensive within-subclade variation, whereas taxa that experience early explosive bursts of lineage accumulation evolve relatively little within-subclade morphological variation. This pattern is also evident within Australian agamids, which have experienced two pulses of lineage diversification, each associated with large drops in within-subclade variability (Figs. 1 and 2). Application of these methods to taxa that use the environment in fundamentally different ways (e.g., herbivorous or fossorial lizards or nonsquamate taxa) is needed to test the broader generality of the strong negative relationship between LDI and MDI.

Each taxon examined here is species-rich and ecologically and phenotypically diverse, but each has a distinctive pattern of evolutionary diversification (*4*): *Anolis* has diversified by subdividing the arboreal habitat (*13*), whereas much of the diversity of *Liolaemus* represents adaptation to different ecophysiological environments from the hot and arid Atacama Desert to Andean peaks more than 5000 meters high (*14*, *15*). Phrynosomatines and Australian agamids have diversified over a similar range of

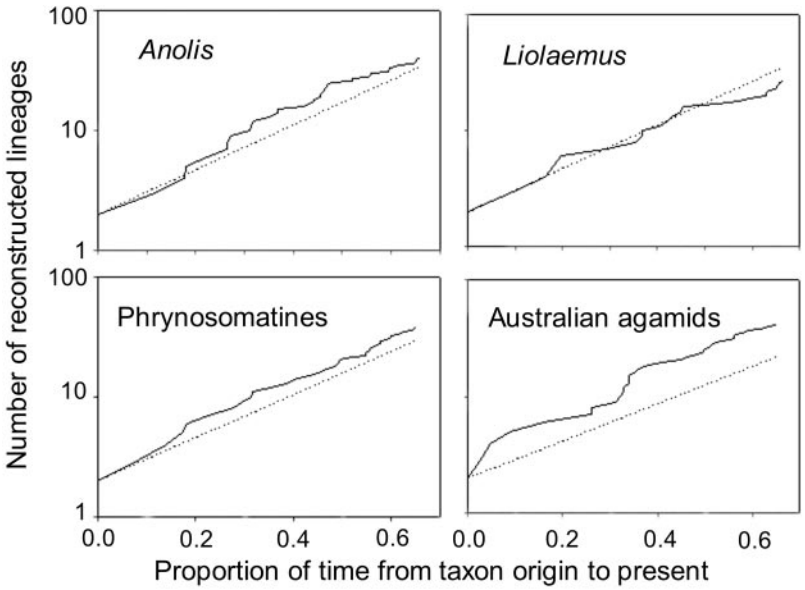

Fig. 1. Lineage accumulation curves for four lizard taxa compared with expectations under the null pure-birth model. Time is expressed as a proportion of the total time since the first cladogenetic event inferred for the taxon. Only the first two-thirds of each phylogeny is shown. Expected curves are obtained using an exponential model with the first branching in a clade set to time = 0 and the number of extant species (Table 1) set to time = 1. Solid line, actual number of reconstructed lineages for the clade; dashed line, expected number of lineages under the null pure-birth model.

Table 1. γ statistics (*20*) and maximum-likelihood estimators (MLE) for the δ statistic (*26*) for the four lizard taxa included in the study. The γ statistic measures whether internal nodes of a phylogeny are closer to the root than would be expected under a model of constant diversification rates (γ = 0). Significant *P* values for a negative value of γ indicate a slowdown of the rate of cladogenesis over the history of the taxon. *P* values were adjusted for level of sampling with the Markov chain constant rates (MCCR) test with 1000 simulations (*20*). The δ statistic measures the extent to which rates of morphological evolution have changed through the history of the group, with values greater than 1 indicating accelerating evolution and values less than 1 indicating deceleration. *P* values were determined from likelihood-ratio tests against a model with constant rates of morphological evolution (*26*). Although MDI and δ statistic values are related ($r = 0.89$), Australian agamids do not show a slowdown in the rates of morphological evolution based on the δ statistic, as would be expected from the disparity through time analysis (Fig. 2). This is likely the result of missing taxa in the phylogeny. The majority of missing species are very closely related and morphologically similar to species that are included in the analysis; not including these species thus masks the overall pattern of a slowdown of morphological evolution. For this reason, we calculated MDI over only the first two-thirds of the disparity-through-time plots.

Clade	No. of species included in phylogeny	Total no. of species in clade	γ statistic	MCCR corrected *P* value	δ statistic (MLE)	*P* value
Anolis	112	147	–3.077	0.005	1.883	0.01
Liolaemus	69	149	–2.253	0.23	3.000	$<<$ 0.0001
Phrynosomatines	71	124	–5.438	$<$ 0.001	1.369	0.16
Australian agamids	69	79	–4.502	$<$ 0.001	1.082	0.86

habitats and, although there are several striking examples of morphological convergence between these taxa, many ecological and morphological forms in one taxon have no counterpart in the other (*17*). Our analyses, by demonstrating differences among the taxa in patterns of lineage accumulation and occupation of morphological space, provide further evidence of among-taxon differences in patterns of diversification.

Despite these diverse evolutionary histories, our analyses reveal an overriding generality: The extent of rapid early diversification and within-clade morphological variability are strongly negatively related ($r = -0.998$). We suggest that this relationship is the result of ecological interactions; taxa that diversify to a large extent early in their histories may fill available ecological space, leaving little opportunity for subsequent ecological diversification within subclades. Conversely, in taxa that accumulate lineages more slowly, subclades have greater opportunity to diversify morphologically, and thus more of a taxon's disparity is partitioned within, rather than among, subclades. Three lines of evidence give credence to this hypothesis. First, strong interspecific competition occurs among extant members of these taxa (*13*, *18*, *27*); second, in the absence of sympatric taxon members, species experience ecological release and niche shifts (*13*); and third, geographic overlap of major subclades of *Liolaemus* is substantially less than that of the other three clades (*28*), and thus subclades of *Liolaemus* may have had the opportunity to diversify independently of each other to a greater extent than did the other taxa.

Alternatively, the inverse correlation between early cladogenesis and within-subclade morphological variability could be explained by the observation that bursts of cladogenesis are sometimes accompanied by exceptionally great increases in morphological disparity as a result either of ecological opportunity or of the relaxation of genetic constraints (*4*). Consequently, one would expect a taxon that experienced rapid diversification early in its history to partition more variation among subclades, even if subsequent evolution followed a random walk through morphological space, unaffected by ecological interactions. Inferences of ancestral morphologies do not reveal obvious differences among the lizard clades in the disparity present at early stages of diversification, but these results are tentative considering the limitations inherent in inferring ancestral character states deep in a phylogenetic tree (*23*, *24*).

Patterns of morphological disparity through time have been studied extensively with fossil data (*7*, *9*, *29*). These studies show that morphological disparity usually peaks earlier in a clade's history than does species diversity (*7*, *29*). Our neontological approach, by focusing on currently diverse extant taxa and how extant diversity and disparity of these clades arose phylogenetically, establishes a second generality about evolutionary diversification: Taxa whose cladogenesis is concentrated early in their histories partition more of their morphological disparity among, rather than within, subclades. These two rules address different aspects of evolutionary diversification and appear complementary; combined phylogenetic and paleontological studies [e.g., (*30*)] may determine whether both occur simultaneously or whether they describe alternative patterns of evolutionary radiation.

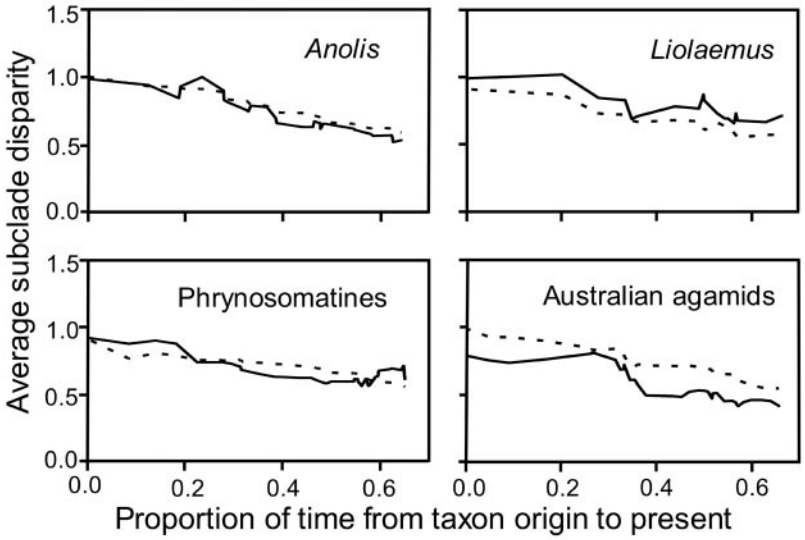

Fig. 2. Relative disparity plots for the lizard taxa compared with expected disparity based on phylogenetic simulations. Average extant disparity at a given point in time is the average disparity of subclades whose ancestral lineages were present at that time relative to the disparity of the entire taxon. The higher the value of relative disparity, the greater the average volume of morphological space occupied by subclades relative to the morphological disparity of the taxon as a whole. Time is expressed as a proportion of the total time after the first cladogenetic event inferred for the taxon. Only the first two-thirds of each phylogeny is shown. Solid line, actual disparity calculated for the clade; dashed line, median expected disparity derived from simulations. Because nested clades tend to contain less morphological disparity than the more inclusive clades to which they belong (*8*), average disparity generally decreases as time approaches the present.

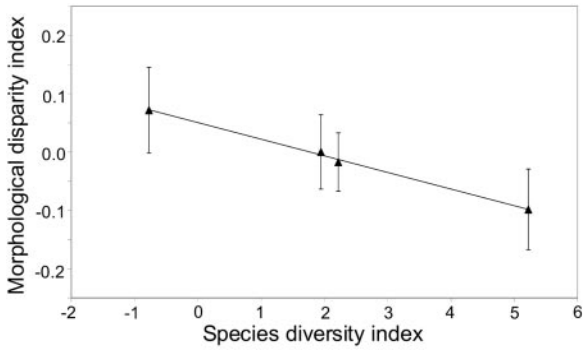

Fig. 3. Relationship between LDI and MDI. Data show a highly significant negative correlation (*19*) ($r = -0.998$, $P = 0.004$). A variety of analyses indicate that the among-clade relationship between LDI and MDI is well-supported and robust to relaxation of assumptions concerning mode of character evolution, sampling, and extinction (*19*) (figs. S6 and S7; 95% confidence limits were established by calculating MDI separately for each of the 1000 simulations of character evolution that were used to calculate MDI for each clade). This result is also significant if γ (corrected for incomplete sampling by subtracting the mean of the γ values in the MCCR test simulations and dividing by the standard deviation of these simulation γ values) and δ values are used for each clade (standardized γ versus δ_{MLE}, $r = 0.97$, $P = 0.03$; in this analysis, the correlation is positive because more negative values of γ reflect a slowdown in diversification, corresponding to larger values of our LDI statistic).

References and Notes

1. T. J. Givnish, K. J. Sytsma, Eds., *Molecular Evolution and Adaptive Radiation* (Cambridge Univ. Press, Cambridge, 1997).
2. D. Schluter, *The Ecology of Adaptive Radiation* (Oxford Univ. Press, New York, 2000).
3. G. G. Simpson, *The Major Features of Evolution* (Columbia Univ. Press, New York, 1953).
4. S. J. Gould, *The Structure of Evolutionary Theory* (Harvard Univ. Press, Cambridge, MA, 2002).
5. S. Conway-Morris, *The Crucible of Creation* (Oxford Univ. Press, Oxford, 1998).
6. S. Nee, A. O. Mooers, P. H. Harvey, *Proc. Natl. Acad. Sci. U.S.A.* **89**, 8322 (1992).
7. M. Foote, *Annu. Rev. Ecol. Syst.* **28**, 129 (1997).
8. M. Foote, *Paleobiology* **19**, 185 (1993).
9. R. A. Fortey, D. E. G. Briggs, M. A. Wills, *Biol. J. Linn. Soc.* **57**, 13 (1996).
10. C. N. Ciampaglio, M. Kemp, D. W. McShea, *Paleobiology* **27**, 695 (2001).

11. T. R. Jackman, A. Larson, K. de Queiroz, J. B. Losos, *Syst. Biol.* **48**, 254 (1999).
12. L. Rüber, D. C. Adams, *J. Evol. Biol.* **14**, 325 (2001).
13. J. B. Losos, *Annu. Rev. Ecol. Syst.* **25**, 467 (1994).
14. J. A. Schulte II, thesis, Washington University (2001).
15. R. Etheridge, *Am. Mus. Novit.* **3142**, 1 (1995).
16. J. Melville, J. A. Schulte II, A. Larson, *J. Exp. Zool.* **291**, 339 (2001).
17. E. R. Pianka, *Ecology and Natural History of Desert Lizards: Analyses of the Ecological Niche and Community Structure* (Princeton Univ. Press, Princeton, NJ, 1986).
18. J. W. Sites Jr., J. W. Archie, C. J. Cole, O. Flores-Villela, *Bull. Am. Mus. Nat. Hist.* **213**, 1 (1992).
19. Materials and methods are available as supporting material on *Science* Online.
20. O. G. Pybus, P. H. Harvey, *Proc. R. Soc. Lond. Ser. B* **267**, 2267 (2000).
21. The latter test assumes equal diversification rates for all lineages in a given time interval, an assumption that may not be justified in these clades; nonetheless, results of the two tests are in strong agreement.
22. J. B. Losos, D. B. Miles, *Am. Nat.* **160**, 147 (2002).
23. D. Schluter, T. Price, A. O. Mooers, D. Ludwig, *Evolution* **51**, 1699 (1997).
24. C. W. Cunningham, K. E. Omland, T. H. Oakley, *Trends Ecol. Evol.* **13**, 361 (1998).
25. T. Garland Jr., A. W. Dickerman, C. M. Janis, J. A. Jones, *Syst. Biol.* **42**, 265 (1993).
26. M. Pagel, *Nature* **401**, 877 (1999).
27. D. C. Smith, *Ecology* **62**, 679 (1981).
28. J. A. Schulte II, J. R. Macey, R. E. Espinoza, A. Larson, *Biol. J. Linn. Soc.* **69**, 75 (2000).
29. M. A. Wills, in *Fossils, Phylogeny, and Form*, J. M. Adrain, G. D. Edgecombe, B. S. Lieberman, Eds. (Kluwer, New York, 2001), pp. 55–144.
30. P. J. Wagner, *Paleobiology* **21**, 410 (1995).

31. This research was supported by the National Science Foundation and the National Center for Ecological Analysis and Synthesis. We thank M. Foote, R. Glor, T. Jackman, A. Mooers, A. Purvis, and R. Ricklefs for advice and assistance.

Supporting Online Material
www.sciencemag.org/cgi/content/full/301/5635/961/DC1
Materials and Methods
Figs. S1 to S7
Tables S1 and S2

21 March 2003; accepted 16 May 2003

An Expanded Eukaryotic Genetic Code

Jason W. Chin,* T. Ashton Cropp, J. Christopher Anderson, Mridul Mukherji, Zhiwen Zhang, Peter G. Schultz†

We describe a general and rapid route for the addition of unnatural amino acids to the genetic code of *Saccharomyces cerevisiae*. Five amino acids have been incorporated into proteins efficiently and with high fidelity in response to the nonsense codon TAG. The side chains of these amino acids contain a keto group, which can be uniquely modified in vitro and in vivo with a wide range of chemical probes and reagents; a heavy atom–containing amino acid for structural studies; and photocrosslinkers for cellular studies of protein interactions. This methodology not only removes the constraints imposed by the genetic code on our ability to manipulate protein structure and function in yeast, it provides a gateway to the systematic expansion of the genetic codes of multicellular eukaryotes.

Although chemists have developed a powerful array of methods and strategies to synthesize and manipulate small-molecule structures (*1*), our ability to rationally control protein structure and function is still in its infancy. Mutagenesis methods are limited to the common 20 amino acid building blocks, although in a number of cases it has been possible to competitively incorporate close structural analogs of common amino acids throughout the proteome (*2*, *3*). Total synthesis (*4*) and semisynthetic methodologies (*5*, *6*) have made it possible to synthesize peptides and small proteins containing unnatural amino acids but have limited utility with proteins over 10 kD. Biosynthetic methods that involve chemically acylated orthogonal tRNAs (*7*, *8*) have allowed unnatural amino acids to be incorporated into larger proteins, both in vitro (*9*) and in microinjected cells (*10*). However, the stoichiometric nature of chemical acylation severely limits the amount of protein that can be generated. Thus, despite considerable efforts, the properties of proteins, and possibly entire organisms, have been limited throughout evolution by the 20 genetically encoded amino acids [with the rare exceptions of pyrrolysine and selenocysteine (*11*, *12*)].

To overcome this limitation, we recently showed that new components can be added to the protein biosynthetic machinery of the prokaryote *Escherichia coli* (*13*), which make it possible to genetically encode unnatural amino acids in vivo. A number of unnatural amino acids with novel chemical, physical, and biological properties (*14*–*19*) have been incorporated efficiently and selectively into proteins in response to the amber codon TAG. However, because the translational machinery is not well conserved between prokaryotes and eukaryotes is not highly conserved, components of the biosynthetic machinery added to *E. coli* cannot be used to site-specifically incorporate unnatural amino acids into proteins to study or manipulate cellular processes in eukaryotic cells.

Thus, we set out to create translational components that would allow us to expand the number of genetically encoded amino acids in eukaryotic cells. *Saccharomyces cerevisiae* was chosen as the initial eukaryotic host organism, because it is a useful model eukaryote, genetic manipulations are facile (*20*), and its translational machinery is highly homologous to that of higher eukaryotes (*21*). The addition of new building blocks to the *S. cerevisiae* genetic code requires a unique codon, tRNA, and aminoacyl–tRNA synthetase (aa RS) that do not cross-react with any components of the yeast translational machinery (*22*–*24*). One candidate orthogonal pair is the amber suppressor tyrosyl–tRNA synthetase–$tRNA_{CUA}$ pair from *E. coli* (*25*, *26*). *E. coli* tyrosyl–tRNA synthetase (TyrRS) efficiently aminoacylates *E. coli* $tRNA_{CUA}$ when both are genetically encoded in *S. cerevisiae* but does not aminoacylate *S. cerevisiae* cytoplasmic tRNAs (*27*, *28*). In addition, *E. coli* tyrosyl $tRNA_{CUA}$ is a poor substrate for *S. cerevisiae* aminoacyl–tRNA synthetases (*29*) but is processed and exported from the nucleus to the cytoplasm (*30*) and functions efficiently in protein translation in *S. cerevisiae* (*27*–*29*). Moreover, *E. coli* TyrRS does not have an editing mechanism and therefore should not proofread an unnatural amino acid ligated to the tRNA.

To alter the amino acid specificity of the orthogonal TyrRS so that it aminoacylates $tRNA_{CUA}$ with a desired unnatural amino acid and none of the endogenous amino acids, we generated a large library of TyrRS mutants and subjected it to a genetic selection (*31*). On the basis of the crystal structure of the homologous TyrRS from *Bacillus stearothermophilus* (*32*), five residues (Fig. 1A) in the active site of *E. coli* TyrRS that are within 6.5 Å of the para position of the aryl ring of bound tyrosine were randomly mutated. A selection strain of *S. cerevisiae* [MaV203: pGADGAL4 (2 TAG) (*33*–*35*)] was transformed with the library to afford 10^8 independent transformants and grown in the presence of 1 mM unnatural amino acid (Fig. 2C). Suppression of two permissive amber codons in the transcriptional activator GAL4 leads to the production of full-length GAL4 (*36*) and the transcriptional activation of the GAL4-

Department of Chemistry and Skaggs Institute for Chemical Biology, Scripps Research Institute, 10550 North Torrey Pines Road, La Jolla, CA 92037, USA.

*Present address: Medical Research Council Laboratory of Molecular Biology, Hills Road, Cambridge CB2 2QH, UK.

†To whom correspondence should be addressed. E-mail: Schultz@scripps.edu